with six different width ratios and four gap ratios, depend on free stream velocities (15, 20 and 26 m/s). In this study, all the computational data are calculated and compared to each other as well as some of these results are discussed with respect to the experimental data [3].

5.1 Results for Rear Body Alone

For rear body alone the numerical stream velocity contours (left column) are given in Figures 3a, 3b, and 3c. The orange area corresponds to the free-stream velocities (15, 20 and 26 m/s), respectively. The red area indicates high velocity, while the blue area shows the low velocity. The stream velocity contours clearly indicate that the wake zone behind the rear body, and consequently the pressure drag are increased as the free stream velocity increased. The boundary layer separation occurs at the leading edges of the rear body, which fed in strong, alternative eddies resulting in high wake zone behind the body, and consequently in high drag coefficient.

Figures 3d, 3e and 3f, shows the corresponding pressure coefficient contours (right column) for the three different velocities. It is clear that, the red area indicated the excess (high positive) pressure due to the stagnation of the approaching flow on the rear body front face. Whereas, the blue area indicate the suction (high negative) pressure which occurs due to the separation of boundary layers at the sharp corners resulting in large wake zone behind the body. Consequently the difference in these two pressures caused the pressure drag. The numerical values of (CDo) for the rear body alone at different velocities (V=15, 20 and 26m/s) are (1.213, 1.214 and 1.216), respectively. The numerical results with experimental data [3] are compared, for rear body alone drag coefficients (CDo) at three different velocities as shown in Table (1). These results show that the percentage differences (error) between the numerical and experimental [3], is (5%) occurs at velocity (v=15m/s). Whereas, the differences (12% and 14 %), for the other velocities 20 and 26 m/sec respectively.

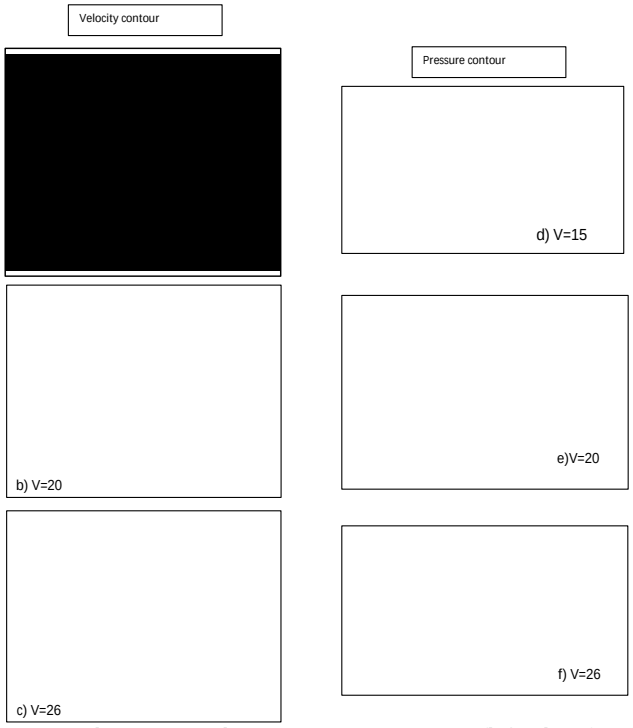

Figure 3: Flow stream velocity components contours (left column) and pressure coefficient CP contours (right column) at different velocities (V=15, 20 and 26 m/s) for the rear body only.

Table 1: Drag coefficient for rear body alone for three different velocities.

Case	Drag coefficient(C_{Do}) for rear body alone		
	V_1=15 m/s	V_2=20 m/s	V_3=26 m/s
ANSYS- FLUNET	1.213	1.214	1.216
Experimental [3]	1.28	1.39	1.42
Difference (%)	5	12	14

5.2 Results for Front-Rear Body combinations

Figure 4 shows the variation of stream velocity for front-rear body combinations, for different width ratios (b1/b2=0.25, 0.37, 0.50, 0.62, 0.75 and 1.0) and g/b2 = 0.5 at velocity 15m/s. In figure (4) shows how the geometry (i.e. width ratio) effect on the stream velocity and wake zone, red area corresponding to high velocity and low pressure, while the blue area gives low velocity and high pressure. The optimum combination is marked by [*]. Each combination will discussed and combative to each other separately.

At b1/b2=0.25, Figure 4a, for small width ratio the boundary layer separated from the front body will reattachment to the rear body face , and again separated from the rear body corners. The wake zone is started on or near the shoulders. Consequently, result in open up wake zone and high drag coefficient.

In figure 4b, b1/b2= 0.37, the flow is similar to this in b1/b2=0.25. But, it may be seen from the velocity contours that the boundary layers separation from the front body have a tendency to reattachment to the shoulder of rear body. Resulting in small wake zone compared with that take place in combination b1/b2=0.25.

For the b1/b2=0.50 and 0.62, figure 4c and 4d, these geometry combination is near to the optimum case figure 4e, (b1 */b2=0.75 and g */b2=0.5), the boundary layers separated are very close to the shoulder of rear body, but still appears unsteadiness in separated boundary layers. For combination b1/b2=0.75, figure 4e, in this case the flow is steady and the boundary layers separated from the front body are very thin and reattachment at the rear body shoulder, and consequently resulting in good shielding effect. These combination (b1 */b2=0.75 and g */b2=0.5) is the optimum case. The minimum drag coefficient (CD=0.604) achieved in this case, is lower by (48%) than the drag coefficient for rear body alone. For large combination width ratio b1/b2=1.0, figure 4f, the separated boundary layers are on the sides of the rear body. Resulting in high drag coefficient compared with the others combinations.

In Figure (5a-5f) show the pressure coefficient variation around the six different width ratios (b1/b2) for gap ratio (g/b2=0.5) at speed (V=15m/s). It can be seen that a remarkable contrast in pressure distribution between the different combinations. However, for small width ratio (b1/b2=0.25 and 0.37), it observe that the face of the rear body is exerted to high pressure (+Cp) which is represented by yellow area, due to the flow separated from the front body strike the face and become stagnation, and again separated from the face of rear body, accelerated at the upper and lower sides of the rear body, causing in pressure drop (-Cp) which is represented by a blue area as shown in figures 5a and 5b.

For a combinations (b1/b2=0.50 and 0.62), the entire rear body is subjected to low pressure coefficient and represented by blue area, while the face of front body is subjected to high pressure coefficient, as shown in figures 5c and 5d.

By compared with the optimum case (b1 */b2=0.75 and g */b2=0.5) shown in figure 5e, the rear body front face is subjected to very low pressure (-Cp) which is represented by blue area. While the other sides such as upper and lower surfaces are subjected to low pressure. This fact can be interpreted in term of boundary layers, where it separated from the front body leading edges is reattachment to the corners of the front face of rear body, resulting in small wake zone behind the rear bod and consequently in low drag coefficient.

For large width ratio (b1/b2=1.0), there is a high positive pressure (+Cp) on the face of front body and entire rear body are become under negative pressure, as shown in figure 5f. Therefore, the drag coefficient is more than the rear body alone.

The variation of drag coefficient ratio (CD/CDo) for each combination with gap ratio is plotted for Reynolds number (1-1.8) × 105 in figures (6a-6f). It is observe that the trend of drag coefficient ratio is similar for low width ratios (b1/b2=0.25 and 0.37) as illustrated in figures 6a and 6b and the drag coefficient ratio decreased as gap ratio increased. This can be explained as the separated boundary layer has a tendency to reattachment on the corners of rear body. The minimum drag coefficient can be achieved at the optimum combination (b1 */b2=0.75 and g */b2=0.5) as shown in figure 6e. Optimum shielding effect occurs at this combination, the separation boundary layers from the front body are reattachment to or very close to the rear body leading edges.

In figures (7a, 7b, 7c and 7d), show the stream velocity components contour for the optimum width ratio (b_1^*/b_2 =0.75) at different gap ratios (g/b2=0.25, 0.50, 0.75 and 1.0). It is evident that, the wake zone behind the optimum combination is steadier and smaller in size, as shown in figure (7c) when compared with the other combinations figures 7a, 7b and 7d. The reason for this behavior can be attributed to the shielding effect.
The evaluated numerical results of the minimum drag coefficient (C_D^*) for each combination (b_1^*/b_2) and the corresponding optimum gap ratio (g^*/b_2) at which it occurs for three different velocity (V=15, 20 and 26 m/s) are displayed in Table (2).

The percentage drag reduction variation with width ratio (b1/b2) is shown in figure (8), for three different velocities. The behavior exhibited is similar for all the simulated velocities. The maximum reduction in aerodynamic drag coefficient can be achieved with optimum combination (b1 */b2=0.75 and g */b2=0.5) at velocity V=15m/s. Compering with the other optimum configurations, the result is 75% more than that for the same optimum combination but at a velocity V=20m/sec. Although, the above results show that a considerable drag reduction obtained for a certain optimum (front-rear body) configurations, there are some cases other than the optimum results with less drag reduction. This can be attributed to the separated layers from the front body (square plate) are not reattach smoothly to the shoulders of the rear body, and also

The evaluated numerical results for optimum drag coefficient (C_D^*) which is obtained at corresponding velocity variation with the Reynolds number, are shown in figure (9). Further, the numerical result of (C_D^*) from the present work are compared with the experiment data [3] with slightly deviation 15% for low velocity (V=15m/s). It can be seen that, as the Reynolds number increased beyond the critical number (1-1.8) ×105, the rate of deviation increased.

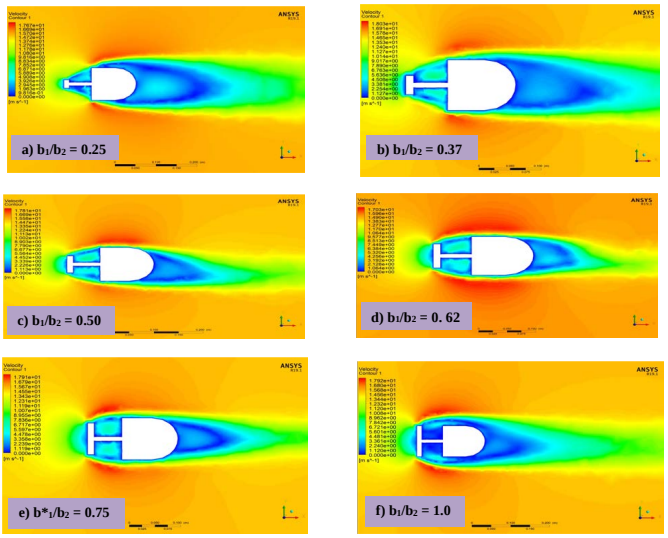

Figure 4: Flow stream velocity components contours for different width ratios (b_1/b_2=0.25, 0.37, 0.50, 0.62, 0.75 and 1.0) at gap ratio g/b_2=0.5 and velocity V=15 m/s.

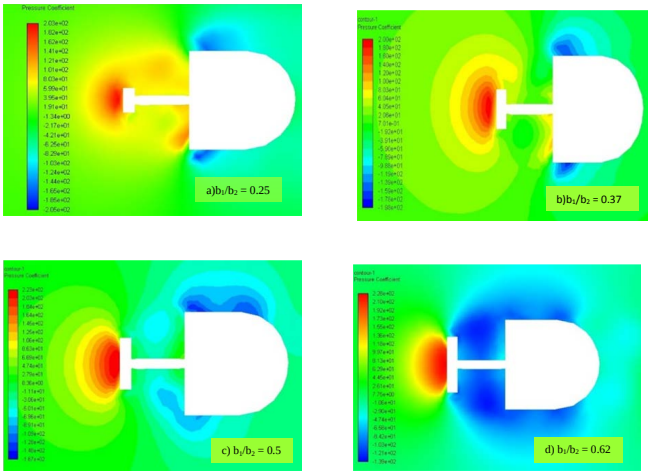

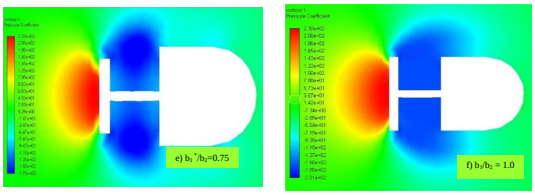

Figure 5: Pressure distribution contours for different width ratios (b_1/b_2=0.25, 0.37, 0.50, 0.62, 0.75 and 1.0) at gap ratio g/b_2=0.5 and velocity V=15 m/s.

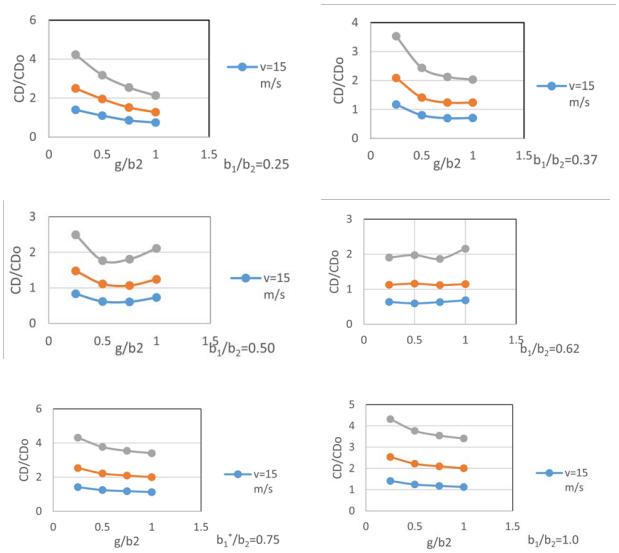

Figure 6: Shows the drag coefficient ratio for b1/b2=0.25, b1/b2=0.37, b1/b2=0.5, b1/b2=0.62, b1/b2=0.75 and b1/b2=1.0 respectively for different velocities

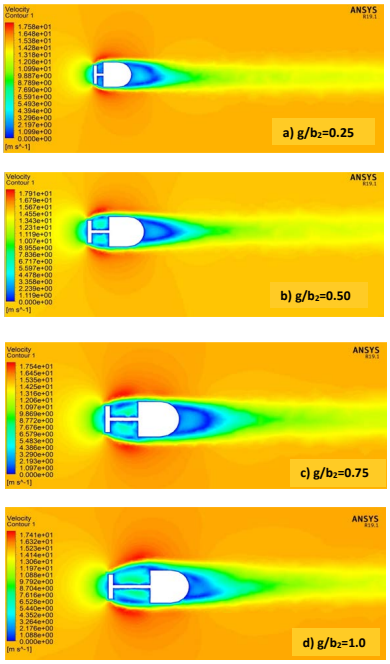

Figure 7: stream velocity components contours for b1/b2=0.75 for different gap ratio g/b2= 0.25, 0.50, 0.75 and 1.0, at velocity (V=15m/s).

Table 2: Optimum drag coefficient (C_D^*) for each combination (b_1^*/b_2) and the gap ratio (g^*/b_2) in which it occurs, for three tested speed.

No.	b_1^*/b_2	g^*/b_2	Optimum Drag coefficient (C_D^*)		
			V_1=15m/s	V_2=20m/s	V_3=26m/s
1	0.25	1.0	0.7410	1.2738	2.1284
2	0.37	0.75	0.6987	1.2402	2.1246
3	0.50	0.75	0.6087	1.0649	1.8056
4	0.62	0.75	0.6338	1.1201	1.8655
5	0.75	0.5	0.6045	1.0651	1.8036
6	1.0	0.75	1.1831	2.0997	3.2381

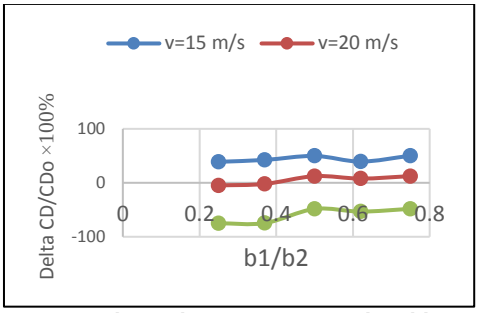

Figure 8: Percentage drag reduction variation with width ratio b1/b2 at three different velocities.

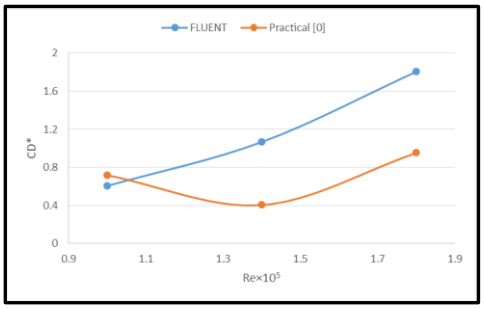

Figure 9: Comparison of variation optimum drag coefficient with Reynolds number for numerically obtained with experimental results [3].

6. CONCLUSIONS

CFD simulation results of 3D, unsteady and incompressible flow around the rear body alone and for different geometrical combinations (width and gap ratios) are discussed. The shielding effects of various square plates placed coaxially as front body upstream of the square flat-faced sharp leading-edges with rounded back rear body, at Reynolds number based on the width of rear body in the range (1-1.8) $\times 10^5$ are presented in this study. It is possible to conclude the following:

1. Based on numerical simulation, the optimum combination was achieved with ($b_1{}^*/b_2$= 0.75 and g^*/b_2= 0.5). Resulting in drag reduction 48% and 12% for the speeds 15 and 20 m/s, respectively.
2. The other investigated combinations give reduction in drag coefficient of (2-10)% ,which is consider low when compared with the drag reduction at the optimum combination.
3. Although the above conclude values show a considerable drag reduction for optimum case, there are some combinations obtained drag more than the rear body alone, resulting in negative percentage drag reduction.
4. The numerical results show that a good agreement with the experimental results that mention in[3], the difference in drag coefficient for rear body alone are 5%, 8% and 14% for the speeds 15, 20 and 26 m/s, respectively.
5. **NOMENCLATURE**
6. D: Drag force; $D = \frac{1}{2}\rho V_\infty^2 A C_D$
7. CD: Drag coefficient; $C_D = \frac{D}{1/2\,\rho\, V_\infty^2 A}$
8. CP: Pressure coefficient; $C_P = \frac{P-P_\infty}{q_\infty}$
9. q_∞: Free stream dynamic pressure; $q_\infty = \frac{1}{2}\rho V_\infty^2$
10. V_∞ : Free stream velocity
11. A: Rear body cross-sectional area; A=b2×b2
12. ρ - Air density =1.225 (kg/m3)
13. P: local static pressure on rear body
14. P_∞: Static pressure in free stream
15. b1, b2: width of front body and rear body, respectively
16. b_1^*/b_2: Optimum front body to rear body width ratio
17. g: Gap between front body and face of rear body
18. g^*/b_2: Optimum gap ratio for a given b_1^*/b_2
19. CDo: Drag coefficient of rear body alone

REFERENCES

[1] Hoerner, S. F. 1965. "Fluid Dynamic Drag" 2nd ed.,.

[2] FLUENT. 2018. Inc., ANSYS FLUENT 19.1 Theory Guide.

[3] Khalid M. Sowoud and Rathakrishnan.E . . 1996. "Front Body Effects on Drag and Flow field of a Three-Dimensional Noncircular Cylinder". AIAA Journal, Vol. 31, No.7, PP.1345-1347.

[4] Xuyong Ying, Fuyon Xu, and Zhe Zhang. 2012. "Numerical Simulation and Visualization of flow Around Rectangular Bluff Bodies". The Seventh International Colloquium on Bluff Body Aerodynamics and Application, September 2-6.

[5] A.K. Saha, G. Biswas, K. Muralidhar. 2003. "Three- dimensional study of flow past square cylinder at low Reynolds number". International Journal of Heat and Fluid Flow, 24, 54-66.

[6] Veeralkumar Thakur, Tarun Yadav, and Dr.Rajiv B.. 2017. "Drag Optimization of Bluff Bodies Using CFD for Aerodynamic Applications". International Journal of Computational Engineering Research (IJCER), ISSN 2250-3005, Vol.07, Issue 04.

[7] Rathakrishnan.E.. 1999. "Effect of Splitter Plate on Bluff Body Drag", AIAA Journal, Vol. 37, No.9, PP. 1125-1126.

[8] V. Suresh, C. Senthilkumar, S. Nadaraja Pillai andS. Arunvinthan. 2015. "Fore body Effect on Bluff Body Drag Reduction at Low Reynolds Number" International Journal of Applied Engineering Research, ISSN 0973-4562 Vol. 10 No.33.

[9] Sercan Yagmur, Sercan Dogan, Muharrem H., Eyub Canli, Muammer Ozgoren. 2015. " Experimental and Numerical Investigation of Flow Structures around Cylindrical Bluff Bodies" Owned by the authors, published by EDP Sciences, EPJ Web of Conferences,92,02113.

[10] Saurabh Banga, Md. Zunaid, Naushad Ahmad Ansari, Sagar Sharma, Rohit Singh Dungriyal. 2015., "CFD Simulation of Flow around External Vehicle: Ahmed Body" Journal of Mechanical and Civil Engineering (IOSR-JMCE) e-ISSN: 2278-1684, P-ISSN: 2320-334X, Volume 12, Issue 4 Ver. III (Jul. - Aug. 2015), PP. 87-94.

[11] Koneig K. and Roshko A. 1985. "An Experimental Study of geometrical effects on the drag and flow field of two bluff bodies separated by a gap", Journal of fluid mechanics, Vol.156, PP. 167-204.

[12] Kostadin Filipov, Sonia Tabakova, "Numerical simulation of the flow around two bluff bodies separated by a gap".https://www. researchgate.net/ publication/ 313752642, (20